Research Article

Investigation of Discretionary Lane-Changing Decisions: Insights From the Third Generation Simulation (TGSIM) Dataset

Yanlin Zhang[1] iD, **Alireza Talebpour**[1] iD, **Hani S. Mahmassani**[2] iD, and **Samer H. Hamdar**[3] iD

Abstract

The data-driven characterization of discretionary lane-changing behaviors has traditionally been hindered by the scarcity of high-resolution data that can precisely record lateral movements. In this study, we conducted an exploratory investigation leveraging the Third Generation Simulation (TGSIM) dataset to advance our understanding of discretionary lane-changing behaviors. In this paper, we developed a discretionary lane-changing extraction pipeline and scrutinized crucial factors such as gaps and relative speeds in leading and following directions. A dynamic time warping (DTW) analysis was performed to quantify the difference between any pair of lane-changing behaviors, and an affinity propagation (AP) clustering, evaluated on normalized DTW distance, was conducted. Our results yielded five clusters based on lead and lag gaps, enabling us to categorize lane-changing behaviors into aggressive, neutral, and cautious for both leading and following directions. Clustering based on relative speeds revealed two distinct groups of lane-changing behaviors, one representing overtaking and the other indicative of transitioning into a lane with stable and homogenous speed. The proposed DTW analysis, in conjunction with AP clustering, demonstrated promising potential in categorizing and characterizing lane-changing behaviors. Additionally, this approach can be readily adapted to analyze any driving behavior.

Lane-changing and car-following behaviors are the two crucial elements of microscopic traffic flow theories; while car-following only addresses longitudinal movements, lane-changing behaviors involve both lateral and longitudinal maneuvers. Despite the extensive research on car-following behaviors over the years, lane-changing behaviors have garnered interest in the past two decades (*1*). This recent attention is attributed to the growing evidence of lane changing's adverse effects on traffic safety (*2, 3*), traffic flow oscillation (*4–7*), and capacity drop (*8*).

In light of the influence of lane-changing behavior on traffic safety, efficiency, and stability, there has been a swift increase in attempts to model lane-changing. Yang and Koutsopoulos (*9*) was one of the pioneers in modeling lane-changing behaviors by extending Gipps' car-following model (*10*) and implemented it into the microscopic traffic simulator, MITSIM. Then Kesting et al.

(*11*) proposed the minimizing overall braking induced by lane changes (MOBIL) model by simplifying the anticipated advantages and disadvantages of lane-changing as single-lane accelerations, which can be integrated with the intelligent driver's model (IDM) (*12*). Another line of modeling lane-changing is based on discrete choice models. Ahmed et al. (*13*) is one of the earliest works defining a utility function for lane-changing behavior. Generally, lane-changing behaviors are categorized as either

[1]Department of Civil and Environmental Engineering, University of Illinois at Urbana-Champaign, Urbana, IL
[2]Northwestern University Transportation Center, Evanston, IL
[3]Department of Civil and Environmental Engineering, George Washington University, Washington, DC

Corresponding Author:
Alireza Talebpour, ataleb@illinois.edu

"discretionary" or "mandatory" (*1*). The primary intent behind a discretionary lane change is to choose a better driving condition, whereas the key incentive for a mandatory lane change is to arrive at the destination. Toledo et al. (*14*) developed a discrete choice framework capturing the trade-off between mandatory and discretionary lane changes with a single utility function. As lane-changing behaviors can be regarded as a competition and cooperation between the lane-changing and surrounding vehicles, Kita (*15*) first formally formulated merging with game theory to explain the real-world merging and giveaway behaviorally. Following similar strategies, Ban (*16*) then proposed robust payoff matrices for defining the strategies. As communication technology enhanced the connectivity among vehicles, Talebpour et al. (*17*) pioneered the effort in game-theoretic modeling lane-changing behaviors in a connected environment. More recent work by Ali et al. (*18*) extended Talebpour et al. (*17*)'s previous work and utilized an advanced driving simulator to collect high-quality vehicle trajectory data for the connected environment.

Furthermore, data-driven analysis of lane-changing behaviors has built a presence in the literature as sensing technology advances and data becomes more accessible, such as naturalistic driving data and trajectory data. Keyvan-Ekbatani et al. (*19*) conducted a naturalistic driving experiment combined with an interview-based study, which categorized lane change decision processes and highlighted diverse driving strategies during these maneuvers. Knoop et al. (*20*) further advanced this study by examining lane-changing behavior on highways through an online survey using video clips, revealing various lane choice strategies adopted by drivers. In a similar vein, Zhang et al. (*21*) proposed a graph-based hidden Markov model to analyze lane-changing behaviors under different traffic conditions using the INTERACTION dataset (*22*), indicating the existence of multiple dynamic interaction patterns in lane changes. Similarly, Yang et al. (*23*) investigated the gap and relative speed based on naturalistic driving data collected from Shanghai, China, and results showed that gaps are significantly affected by surrounding environments. However, this dataset only contains driving data from 60 drivers. Das et al. (*24*) investigated gaps in lane-changing with a much more comprehensive dataset, the Strategic Highway Research Program 2 (SHRP 2), and demonstrated that different factors, including relative speed, traffic conditions, and acceleration, will influence gap acceptance decisions. However, such efforts in analyzing lane-changing behavior are hampered by the complication and difficulty of accurately capturing the longitudinal and lateral position of the lane-changing and surrounding vehicles and identifying the lane boundaries from a naturalistic driving dataset.

To further enhance the understanding of lane-changing behaviors, vehicle trajectory data has become essential, and these datasets fall into three primary categories based on collection methodology:

(i)   Infrastructure based videography: the Next Generation Simulation (NGSIM) (*25*) and I-24 MOTION (*26*) datasets utilize this approach, involving cameras fixed to infrastructure elements like overpasses and buildings. This method can capture detailed traffic flow from multiple angles but requires complex data fusion and interpolation because of overlapping fields of view and stationary recording positions. Wang et al. (*27*) utilized the NGSIM (*25*) dataset and designed heuristic rules to extract discretionary lane changes. Later, Li et al. (*28*) coupled a control model with trajectories to infer common discretionary lane change steering characteristics from NGSIM data. However, researchers are advised not to place excessive trust in the lateral position data provided in the raw NGSIM database, and Coifman and Li (*29*) indicated that refinement on the lateral position from the NGSIM dataset is needed.

(ii) Fixed location aerial videography: the HighD (*30*) and pNEUMA (*31*) datasets employed this method, offering a direct trajectory extraction process. However, the HighD (*30*) dataset's limited coverage and Germany's left-only overtaking restrictions may skew the analysis of lane-changing behaviors. In contrast, pNEUMA's (*31*) focus on urban arterial roads and intersections presents a different set of behavioral dynamics.

(iii) Moving aerial videography: the TGSIM dataset utilizes this approach, where a helicopter follows vehicles, enabling the collection of extended trajectories and detailed behavioral analysis. This method overcomes the limitations of fixed location and infrastructure-based methods by providing comprehensive coverage and precise lane assignments crucial for capturing traffic flow dynamics.

One missing aspect from the previous studies is the categorization and characterization of discretionary lane-changing behaviors based on real-world data, and the critical bottleneck that impedes development in analyzing lane-changing behaviors is the lack of abundant and accurate datasets that can capture lateral movements accurately in traffic flow. Therefore, the objective of this paper is to conduct an exploratory investigation into

discretionary lane-changing characteristics with the TGSIM dataset (32) and gain insights on how different types of lane-changing maneuvers should be categorized. These findings can provide insights into modeling lane-changing behavior under different traffic states and improve microscopic traffic simulation's soundness.

The paper is organized as follows. The next section elaborates on the data preparation steps, followed by the methodologies used in this study: a dynamic time warping (DTW) analysis on lane-changing behaviors and an affinity propagation (AP) clustering method based on the previous DTW analysis. This paper proceeds with a section presenting the results of characterizing lane-changing behaviors with gaps and relative speeds. Finally, this paper is summarized with some conclusions and discussions.

Data Preparation

This section will first briefly introduce the TGSIM dataset and then describe the extraction process of lane-changing cases, followed by presenting some descriptive analysis of the lane-changing measurements and finally, perform hypothesis tests to justify the benefit of splitting the behavior measurements into leading and following when categorizing and characterizing discretionary lane-changing behaviors.

The data used in this paper was collected from a 3-mi segment on I-294 near Hinsdale, IL (one of Chicago's suburbs), using the moving aerial videography method (i.e., a helicopter following the probe vehicles). Data collection occurred in October 2021 during a peak hour between 3 to 5 p.m., and involved a fleet of three adaptive cruise control (ACC) operated vehicles. Unlike previous studies that faced constraints with data collection volume, continuous data was captured by a helicopter equipped with a RED camera at 30 frames per second at 8K resolution following the vehicles at 300 m. The conditions varied between sunny and cloudy. Data collection encompassed a sequence of vehicles operating with ACC in a platoon-like formation, which is frequently segmented because of large gaps, reflecting naturalistic traffic flow. In addition to the aerial-based videos, data from on-board Global Positioning System (GPS) + Inertial measurement unit (IMU) systems were collected to ensure accuracy in trajectory extraction and aid in data verification. The dataset contains 10 experiment runs, each covering four lanes in the same direction. By introducing the idea of "auxiliary lanes" and excluding all the movements from or toward the outside of the four lanes on the main traffic, only the lane changes among the four lanes in the mainstream are considered in this study. Since the merging from on-ramp and diverging toward off-ramp cases are

removed, all the lane changes are regarded as discretionary lane changes in this study. Ammourah et al. (32) has more information on data collection trajectory extraction in detail.

One advantage of TGSIM is that all the boundaries of lanes were carefully marked, and each trajectory point was assigned a lane index after trajectory extraction. As TGSIM data used the center of a vehicle as the proxy of its location, when the lane index changes for the same vehicle index, the center of this vehicle passes the lane markings. According to recent work by Ali et al. (33), a time window of 6 s is preferable for evaluating lane-changing models. Thus, this paper took 3 s before and 3 s after the lane index changes for a vehicle, therefore each lane-changing case has 6 s of data.

Identifying the leader and follower is essential to calculate gaps and relative speeds. Since a lane index is assigned to each trajectory point, identifying the leader and follower is straightforward during lane-changing. This paper only considers the cases where both the leader and follower interact with the lane-changing vehicle. Therefore, if the longitudinal distance between the leader/follower and the lane-changing vehicle is greater than 500 m when the center of the lane-changing vehicle crosses the lane boundary, the lane-changing case will not be extracted into the final lane-changing dataset. There are 477 lane-changing cases following the extraction method described above, and each case contains 6 s of data. As the timeresolution of theTGSIM data is 0.1 seconds, eachlane-changing behavior measurement for a lane-changing case is represented by atime series consisting of 60 consecutive datapoints, corresponding toa 6-second duration.

Figure 1 is an illustration of a typical lane-changing maneuver, and the definitions from Zheng (1) are utilized as a basis for constructing our lane-changing measurements. The lane-changing vehicle (LCV) changes from the initial lane to the target lane, and the leader (LV) and the follower (FV) are the immediately preceding and following vehicles, respectively. The location of vehicle i at time t is defined as the center of a vehicle, $(x_i(t), y_i(t))$, and this paper denotes the speed of vehicle i at time t as $v_i(t)$ and the length as l_i. Zheng (1) used the front-rear distance to represent gaps; however, the lane-changing cases in the TGSIM dataset involve a wide range of speeds (22.22 m/s to 47.49 m/s), and at higher speeds, a vehicle needs a longer spatial distance to maintain the same time gap, resulting in larger front-rear gaps when measured in meters. For the purpose of characterizing lane-changing decisions in this paper, using spatial gaps will induce bias in measuring the difference between lane-changing cases. Therefore, this paper follows the definition presented by Yang et al. (23) of the lead gap $g_i^{lead}(t)$ and lag gap $g_i^{lag}(t)$ for a lane-changing case j at time t and uses time to represent gaps as follows:

Table 1. Descriptive Statistics of Lane-Changing Decision Parameters

Statistics	Speed (m/s)	Acceleration (m/s²)	Gap (s)		Relative speed (m/s)	
			Lead	Lag	Lead	Lag
Count	28620	28620	28620	28620	28620	28620
Mean	24.22	0.08	2.45	2.76	−0.35	1.44
SD	7.77	1.08	2.26	2.70	3.51	3.70
Min.	1.68	−9.95	0.00	0.01	−22.41	−14.68
25%	19.14	−0.27	0.97	1.05	−2.32	−0.87
50%	25.85	0.06	1.68	1.85	−0.18	1.15
75%	30.10	0.50	3.21	3.57	1.62	3.83
Max.	47.39	12.65	25.43	17.05	16.50	19.93

Note: SD = standard deviation; Min. = minimum; Max. = maximum.
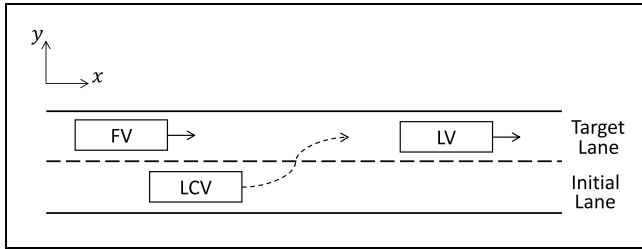
Figure 1. A demonstration of lane-changing decision.
Note: FV = following vehicle; LCV = lane-changing vehicle; LV = leading vehicle.

$$g_j^{\text{lead}}(t) = \frac{x_j^{\text{LV}}(t) - x_j^{\text{LCV}}(t) - l^{,\,\text{LV}}}{v_j^{\text{LCV}}(t)}, \qquad (1)$$

$$g_j^{\text{lag}}(t) = \frac{x_j^{\text{LCV}}(t) - x_j^{\text{FV}}(t) - l^{\text{LCV}}}{v_j^{\text{FV}}}. \qquad (2)$$

The relative speeds are also useful in measuring lane-changing decisions (23) and are defined as follows:

$$\Delta v_j^{\text{lead}}(t) = v_j^{\text{LV}}(t) - v_j^{\text{LCV}}(t), \qquad (3)$$

$$\Delta v_i^{\text{lag}}(t) = v_j^{\text{LCV}}(t) - v_j^{\text{FV}}(t). \qquad (4)$$

Table 1 shows the descriptive statistics of the key parameters influencing lane-changing decisions extracted from the TGSIM I-294 dataset. The average speed of 24.22 m/s suggests a moderate traffic flow, with a significant spread in speeds indicated by the standard deviation of 7.77 m/s. The large standard deviation underscores a diverse range of driving behaviors. The breadth of vehicle speeds, spanning from 1.68 m/s to 47.29 m/s, encompasses a variety of traffic conditions from congested to free-flowing states. The mean acceleration is near-zero, implying steady flow conditions, but the range from −9.95 to 12.65 m/s² indicates occasional rapid changes in speed. The lead and lag gap times, with means of 2.45 and 2.76 s, respectively, hint at drivers' preference for a slightly larger buffer behind them than in front. The negative mean lead relative speed (–0.35 m/s) suggests that lane changes tend to occur when the leading vehicle is traveling at a slower speed than the lane-changing vehicle, while the positive mean lag relative speed (1.44 m/s) indicates a tendency to change lanes into a space where they are faster than the following vehicle. The percentiles provide additional insight into driving behaviors, with the 25% and 75% values delineating the typical range of gap acceptance and relative speeds during lane-changing maneuvers. These insights into gap acceptance and relative speeds during lane changes are critical for understanding the complex dynamics of driver decision-making during lane-changing maneuvers.

Figure 2 displays the joint and marginal distributions of the follower and leader gaps, and these distributions do not appear to be normally distributed and are right-skewed with long tails, rendering the central limit theorem and law of large numbers inapplicable. Figure 3 shows the two relative speeds may share similar standard deviations but differ in the mean value. In line with the theory proposed by Laval (34), such distributions of lead and lag gaps may follow a power-law:

$$P(x; \alpha, x_{\min}) = Cx^{-\alpha} = (\alpha - 1)x_{\min}^{\alpha-1}x^{-\alpha} \qquad (5)$$

where α is the scaling parameter or critical exponent, and x_{min} is the lower bound of x, since the density diverges when $x \to 0$. $C = (\alpha - 1)x_{\min}^{\alpha-1}$ is the normalization constant that ensures $\int_{x_{\min}}^{\infty} Cx^{-\alpha}dx = 1$.

To characterize the long-tail distribution of the lead and lag gaps, the maximum likelihood estimation (MLE) and the likelihood ratio testing (LRT) methods outlined by Clauset et al. (35) are employed, comparing them against log-normal distributions because of their propensity for modeling heavy-tailed data. Therefore, the long-tail distribution of lead and lag gaps are fitted with a log-normal distribution:
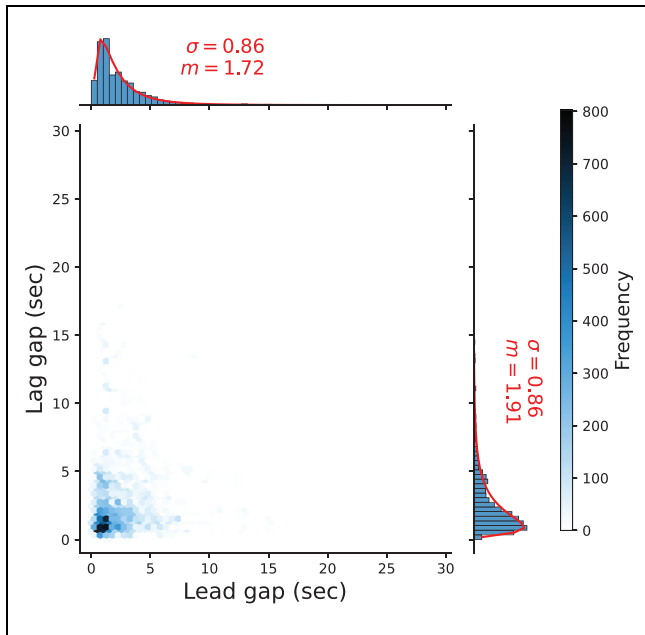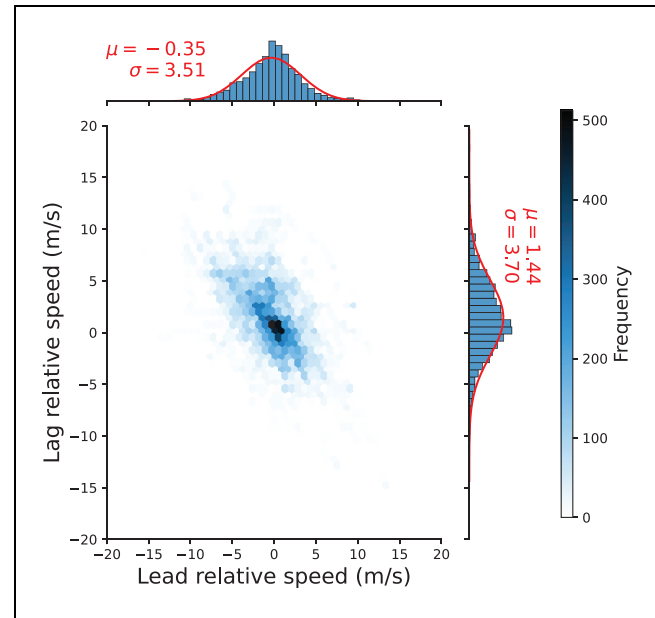
Figure 2. The joint and marginal distribution of lead and lag gaps.
Note: The red curves present the estimated log-normal distribution of the lead and lag gaps.

Figure 3. The distribution of relative speed compared with leader and follower.
Note: The red curves present the estimated normal distribution of the lead and lag relative speeds.

$$P(x; m, \sigma) = \frac{1}{x\sigma\sqrt{2\pi}} \exp\left[\frac{-\ln^2(x/m)}{2\sigma^2}\right] \qquad (6)$$

where m is the scale parameter and the median on the nature scale; σ is the shape parameter and the standard deviation on the log scale.

In the likelihood ratio test, the null hypothesis is that the data follows a power law distribution, while the alternative hypothesis is that the data follows a log-normal distribution. The test results show that the log-normal distribution provided a better fit for both lead and lag gaps. This conclusion is supported by the likelihood ratio test statistics of -14.76 and -122.71, with corresponding significance values of $0.00.$. The negative values of the LRT statistics suggest that the data is more likely to follow the log-normal distribution, and the near-zero significance values provide strong evidence against the null hypothesis. Figure 2 illustrates the estimated log-normal distribution with red lines. This finding implies that, contrary to our initial hypothesis that the lead and lag gaps follow a power law distribution, they are more accurately modeled by a log-normal distribution. This has significant implications for modeling traffic flow and lane-changing behavior. The procedures we followed for this analysis were adapted from the powerlaw package in Python (*36*).

Moreover, the Wilcoxon signed-rank test (*37*) is employed to ascertain the need for separate treatment of lead and lag gaps and relative speeds in modeling lane-changing decisions. The Wilcoxon signed-rank test is a non-parametric equivalent to the paired T-test, suitable for paired samples like our lead and lag gaps at each timestamp. The test yielded statistics of 183279819 and 137820170 for gaps and relative speeds, respectively, with p-values of 0.0000 in both cases. This strongly indicates that lead and lag gaps and relative speeds are drawn from distinct distributions, justifying the separate treatment of leading and following directions in our analysis of lane-changing behavior. The efficacy of the Wilcoxon test in handling heavy-tailed data is corroborated by its application in other domains, such as e-commerce order size analyses (*38*), further validating its robustness for our approach.

For comparison and verification purposes, this paper utilizes the US-101 dataset from NGSIM (*25*). To focus on discretionary lane-changing maneuvers, lane-changing maneuvers involving ramps are excluded, and only lane-changing maneuvers between lanes from lane 1 (the farthest left lane) to lane 5 (the farthest right lane) are considered. Instances where there is no leading or following vehicle in the target lane are not included. From 7:50 a.m. to 8:35 a.m., a total of 783 discretionary lane-changing cases were extracted.

Methodology

This section presents two steps to categorize and characterize the discretionary lane-changing behaviors from real-world trajectory data. The first step is to construct a
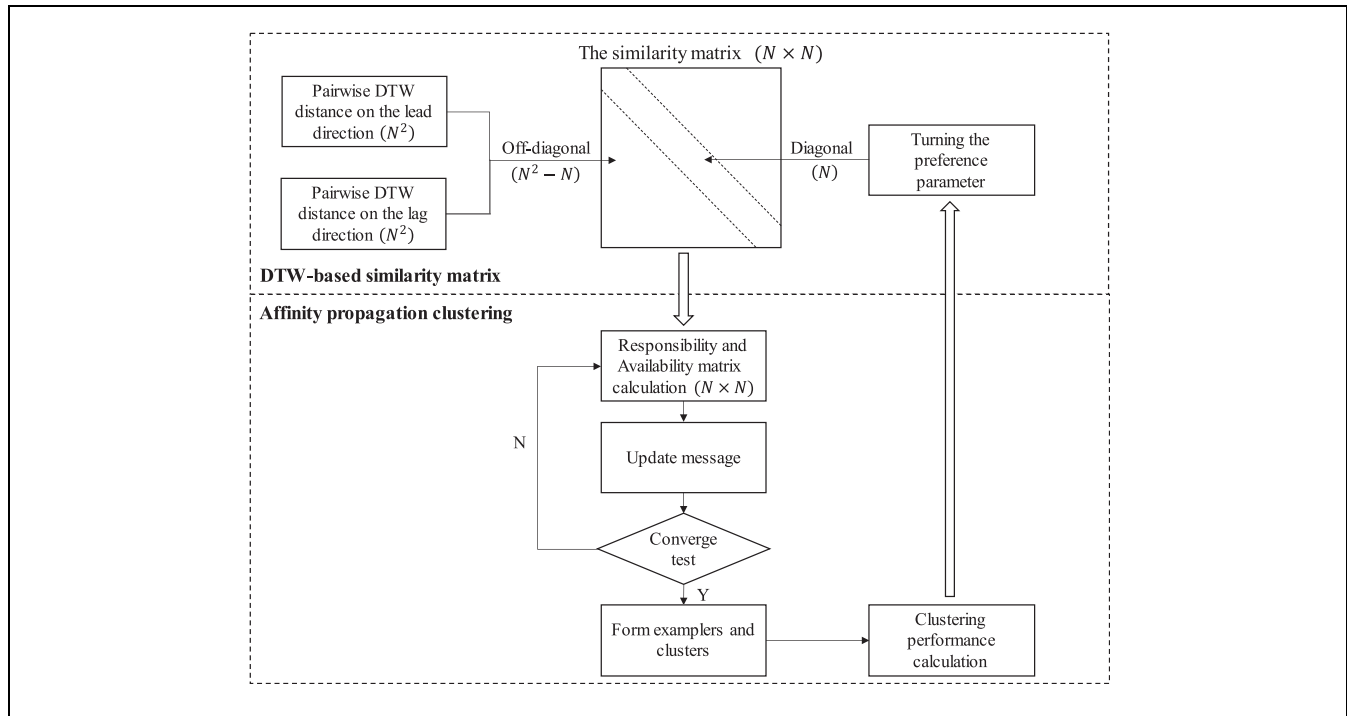
Figure 4. Overview of the proposed methodological framework for lane-changing behavior clustering.

DTW analysis framework to evaluate the similarity between any lane-changing cases, and the second step is to perform affinity clustering based on the DTW similarities to identify different categories in discretionary lane-changing behaviors.

Figure 4 outlines our methodological framework for clustering lane-changing behavior with DTW-based AP clustering. This approach consists of calculating the similarity matrix based on the DTW distance and AP clustering. It initiates the computation with pairwise DTW distances for the off-diagonal elements of the similarity matrix. For the diagonal elements, the preference hyperparameter is iteratively tuned to optimize clustering performance. This iterative process involves a feedback loop where after each clustering iteration, performance metrics are evaluated to adjust the preference parameter. Following the formation of the similarity matrix, the AP algorithm iteratively computes responsibility and availability matrices until convergence is achieved. Upon convergence, exemplars are selected, and clusters are formed. The cycle continues until the most effective hyperparameter value is determined, ensuring that the AP clustering algorithm can distinguish between different behaviors.

DTW Analysis on Lane-Changing Behaviors

The idea of using dynamic programming algorithms to find matching patterns between time series data originated from the seminal work by Bellman and Kalaba (*39*), and was then formally formulated and widely applied in speech recognition by Myers et al. (*40*) and Sakoe and Chiba (*41*). Recent studies by Zhang and Talebpour (*22*) and Hosseini et al. (*42*) that applied DTW analysis to driving behaviors have demonstrated that the method offers a distinct advantage in comparing time series, as it can align sequences of varying lengths and capture meaningful patterns, rendering it an apt choice for driving behavior analysis.

In assessing the difference between two time series of driving behaviors, $A = [a_1, a_2, \ldots, a_m]$ and $B = [b_1, b_2, \ldots, b_n]$, a conventional and intuitive metric is the Euclidean distance (ED), as defined in Rakthanmanon et al. (*43*):

$$\mathrm{ED}(A, B) = \sqrt{\sum_{t=1}^{T} (a_t - b_t)^2} \tag{7}$$

where $T = \min\{m, n\}$ represents the length of the shorter time series

Given that the duration of lane-changing cases in this study is fixed at 6 s, all time series have the same length, with $m = n = 60$. While the ED provides a basic measure of dissimilarity, it may not effectively capture the patterns and alignments among time series, which is essential to clustering analysis. To address this issue, this paper

employs DTW analysis. In DTW, the local cost matrix $D \in \mathbb{R}^{m \times n}$ is defined as

$$D \in \mathbb{R}^{m \times n} : d_{ij} = \| a_i - b_j \|$$
$$= \sqrt{\left(a_i - b_j \right)^2}, i \in [1:m], j \in [1:n] \quad (8)$$

where d_{ij} is an element in the local cost matrix D.

Building on the local cost matrix, the warping path $W = [w_1, w_2, w_3, \ldots, w_k, \ldots, w_K]$ represents a set of mapping relationships between A and B. An element in the warping path $w_k = (i_k, j_k) \in [1:m] \times [1:n]$ means a_{i_k} and b_{j_k} form a pair in the optimal matching.

Then Senin (44) introduced the following formulation:

$$\text{DTW}(A, B) = \min_W \sum_{k=1}^{K} d_{i_k j_k}. \quad (9)$$

where $DTW(A, B)$ is the DTW distance between time series A and B. $d_{i_k j_k}$ is the (i_k, j_k)-th elements in the local cost matrix D.

The constraints are:

$$w_1 = (1, 1), \quad (10)$$

$$w_K = (m, n), \quad (11)$$

$$\left(i' - i \right) \leqslant 1, \forall w_k = (i, j), w_{k+1} = \left(i', j' \right), \quad (12)$$

$$\left(j' - j \right) \leqslant 1, \forall w_k = (i, j), w_{k+1} = \left(i', j' \right), \quad (13)$$

$$\left(i' - i \right) \geqslant 0, \forall w_k = (i, j), w_{k+1} = \left(i', j' \right), \quad (14)$$

$$\left(j' - j \right) \geqslant 0, \forall w_k = (i, j), w_{k+1} = \left(i', j' \right), \quad (15)$$

The six constraints described above embody three fundamental assumptions initially proposed by Sakoe and Chiba (41). These assumptions are as follows: (i) **Boundary assumption :**Equations 10 and 11 guarantee that the warping path begins at the first points and ends at the last points of the two time series, representing an alignment assumption in DTW; (ii) **Continuous assumption:**Equations 12 and 13 ensure a match with neighboring points, indicating that every time step should be included in the optimal warping path; and (iii) **Monotonous assumption:** Equations 14 and 15 preserve the time order and effectively prevent time from moving backward.

It has been proven by Senin (44) that the optimization problem defined by Equations 9 to 15 reduced to a shortest path problem in the cumulative distance matrix $C \in \mathbb{R}^{m \times n}$, which can beefficiently solvedusing dynamic programming.

The pseudo-code for the dynamic programming algorithm in computing the cumulative distance matrix

---

Algorithm 1 CummulativeDistanceMatrix(A, B, D)

```
1: m ← ‖ A ‖
2: n ← ‖ B ‖
3: New array C[1...m, 1...n]
4: Initialize C[1, 1] = 0
5: for i = 1; i≤m; i + + do
6:     C[i, 1] ← C[i − 1, 1] + D[i, 1]
7: end for
8: for j = 1; j≤n; j + + do
9:     C[1, j] ← C[1, j − 1] + D[1, j]
10: end for
11: for i = 1; i≤m; i + + do
12:     for j = 1; j≤n; j + + do
13:         C[i, j] ← D[i, j] + min{C[i − 1, j − 1], C[j − 1, j], C[i, j − 1]}
14:     end for
15: end for
16: Return C
```

$C \in \mathbb{R}^{m \times n}$ described in Senin (44) is presented in Algorithm 1.

It takes $O(mn)$ to compute the local distance matrix D and the cumulative distance matrix C (44). Then given the cumulative distance matrix, the optimal warping path W can be recovered in $O(n)$ time by tracing back from $C[m, n]$ to get the warping path W.

Since the time series measured in this study are identical in length (all lane-changing cases are 6 s), a length-based normalization conducted in Zhang and Talebpour (22) is unnecessary.

Table 2 illustrates a simplified numerical example, elucidating the difference in measuring the difference between two time series data with the DTW distance and the ED. This example derives from a piece-wise linear abstraction of speeds observed in two specific lane-changing cases: one involves vehicle ID = 20 in Run 7, moving from lane 4 to 5, and the other involves a vehicle from ID = 35 in Run 7, moving from lane 4 to 3. Figure 5 visually demonstrates that the ED measures the difference based on corresponding indices, without considering the underlying matching patterns. As computed using the formula in Equation 7, the ED is 6.08 m/s. Conversely, Figure 5 displays how the DTW distance identifies an optimal alignment. Following the definition described in Equation 9, the DTW distance is 8 m/s. It is important to note that both the ED and the DTW distance serve as measures of dissimilarity, not direct measures of physical distance.

To better illustrate the process and output of DTW analysis, the speed of the lane-changing vehicle in two lane-changing cases is taken as a sample. Figure 6, as an exemplification, showcases its accuracy in finding the warping path and, thus, the matching patterns by minimizing the cumulative costs. Figure 7 shows the corresponding matching patterns based on the warping path
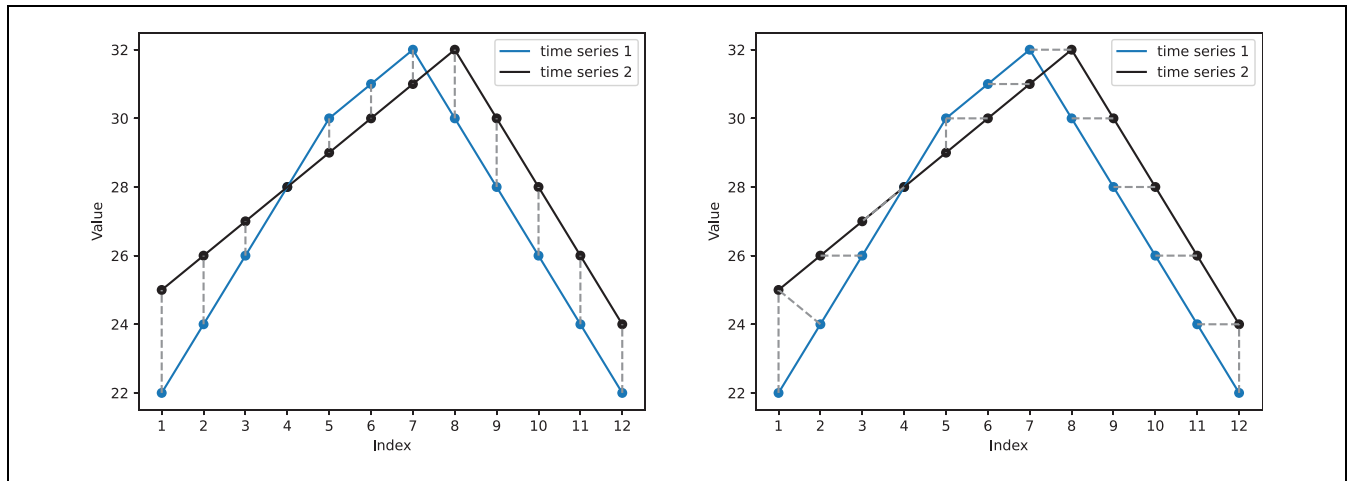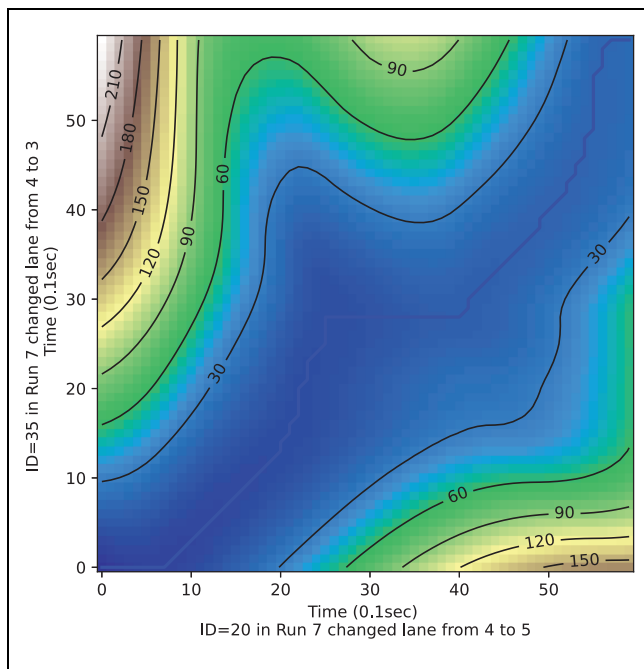
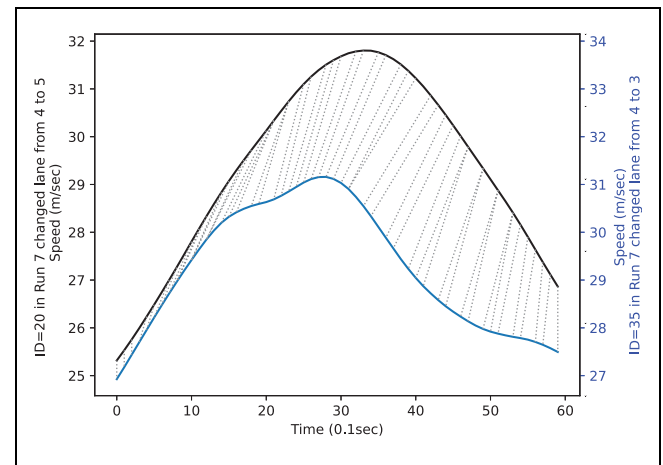**Figure 5.** A comparison of *ED* and *DTW* calculation.

Table 2. Piece-Wise Linear Speed Example for Euclidean Distance and Dynamic Time Warping Calculation

Index	1	2	3	4	5	6	7	8	9	10	11	12
Time series 1(m/s)	22	24	26	28	30	31	32	30	28	26	24	22
Time series 2(m/s)	25	26	27	28	29	30	31	32	30	28	26	24

Figure 6. A demonstration of finding the warping path by solving for the shortest path in the local cost matrix.

Figure 7. A demonstration of matching patterns between data from two speed time series based on dynamic time warping.

the vehicle ID = 35 in Run 7 changing lanes from 4 to 3. The speed axis has an offset of 2 units to illustrate the matching patterns better.

In accordance with the established framework, a DTW distance matrix corresponding to lane-changing behavior measurements can be computed. The obtained difference measurements can subsequently be converted into similarity by inverting the value of each element. These measurements thus serve as an input to the clustering algorithms presented in the following subsection.

shown in dark blue in Figure 6. The black line is the speed for the vehicle ID = 7 in experiment Run 7 when changing lanes from 4 to 5; the blue line is the speed for

AP Clustering Based on DTW

This research aims to categorize discretionary lane-changing behaviors using real-world trajectory data. Current classification standards for lane-changing behaviors are inadequately defined for appropriately labeling the extracted data, underscoring the need for a clustering method. Given the exploratory nature of this study and the indeterminate number of clusters, clustering methods such as k-means (45) and spectral clustering (46), which necessitate prior knowledge of the number of clusters, do not align with the study objectives. Density-based spatial clustering of applications with noise (DBSCAN), another prevalent unsupervised method, is not ideal given its inherent limitation of potentially classifying some data points as outliers not belonging to any cluster (Ester et al. [47]). This runs counter to our aim of achieving a comprehensive categorization of discretionary lane changes across various traffic states. Consequently, we have chosen AP proposed by Frey and Dueck (48) as the clustering method for our analysis because of its suitability for our research needs, providing unbiased categorization of discretionary lane-changing behaviors.

One of the key inputs of AP clustering is the similarity matrix. Inspired by Akl and Valaee's (49) successful implementation of DTW on multi-dimensional acceleration in gesture recognition using AP clustering, this work designed the similarity matrices as follows:

$$S(i,j)^{\mathrm{DTW}} = \begin{cases} -\mathrm{DTW}^2\left(X_i^{\mathrm{lead}}, X_j^{\mathrm{lead}}\right) - \mathrm{DTW}^2\left(X_i^{\mathrm{lag}}, X_j^{\mathrm{lag}}\right), i \neq j \\ p, i = j \end{cases}$$

(16)

where $\mathrm{DTW}\left(X_i^{\mathrm{lead}}, X_j^{\mathrm{lead}}\right)$ and $DTW\left(X_i^{\mathrm{lag}}, X_j^{\mathrm{lag}}\right)$ are the DTW distance for leader- and follower-related factors, respectively. The factors include gaps and relative speed, defined in $\left(X_j^{\mathrm{lead}}, X_j^{\mathrm{lag}}\right) \subset \{\left(G_j^{\mathrm{lead}}, G_j^{\mathrm{lag}}\right),$ $\left(\Delta V_j^{\mathrm{lead}}, \Delta V_j^{\mathrm{lag}}\right)\}$, where $G_j^{\mathrm{lead}} = [g_j^{\mathrm{lead}}(1), g_j^{\mathrm{lead}}(2),$ $\ldots, g_j^{\mathrm{lead}}(n)]$ and $\Delta V_j^{\mathrm{lag}} = [\Delta v_j^{\mathrm{lag}}(1), v_j^{\mathrm{lag}}(2), \ldots, v_j^{\mathrm{lag}}(n)] . p$ is the preference for each data point; points with a larger preference are more likely to be chosen as exemplars. An exemplar means cluster centers (50). Therefore, p should be initialized as an array with identical elements to maintain impartiality during clustering.

In line with our exploration of clustering analysis, the similarity matrix for the base case is constructed using the ED defined in Equation 7 as the metric. This approach allows us to establish a benchmark for comparison with the DTW method, thereby demonstrating the enhanced effectiveness of DTW in capturing the nuanced patterns in time series data. The similarity matrix using ED is defined as follows:

$$S(i,j)^{\mathrm{ED}} = \begin{cases} -\mathrm{ED}^2\left(X_i^{\mathrm{lead}}, X_j^{\mathrm{lead}}\right) - \mathrm{ED}^2\left(X_i^{\mathrm{lag}}, X_j^{\mathrm{lag}}\right), i \neq j \\ q, i = j \end{cases}$$

(17)

where X_j^{lead} and X_j^{lag} retain their previously defined meanings, and q represents the preference parameter. The method for tuning this parameter is detailed in the results section.

AP can be viewed as exchanging messages between the data points and the message, including the responsibilities $r(i, k)$ and availabilities $a(i, k)$ between point i and k. The update function of responsibilities and availabilities are defined as follows (48):

$$r_{\mathrm{new}}(i,k) = \lambda r_{\mathrm{old}}(i,k) + (1 - \lambda)\left(S(i,k) - \max_{j, j \neq k}\{a(i,j) + S(i,j)\}\right)$$

(18)

$$a_{\mathrm{new}}(i,k) = \begin{cases} \lambda a_{\mathrm{old}}(i,k) + (1 - \lambda)\left(\min\{0, r(k,k) + \sum_{j, j \neq i, j \neq k} \max\{0, r(j,k)\}\right), i \neq k \\ \lambda a_{\mathrm{old}}(i,k) + (1 - \lambda)\left(\sum_{j, j \neq k} \max\{0, r(j,k)\}\right), i = k \end{cases}$$

(19)

where λ is a damping factor between 0 and 1. This is to avoid unstable dynamics in practice (48).

The responsibilities and availabilities at any step can be used to identify exemplars. For lane-changing case i, let $k = argmax_j\{a(i,j) + r(i,j)\}$ if $k = i$ then i is an exemplar; and if $k \neq i$, then k is an exemplar for i. Algorithm 2 describes the AP clustering implementation proposed by Frey and Dueck (48). The similarity matrix S is computed based on Equation 17, and preference p is a function of the median of the similarity matrix S—how to determine preference will be discussed in detail in the following results section. Other parameter keep fixed values in this study, including the damping factor $\lambda = 0.5$, the maximum number of iterations, *max_iter* = 200, and the number of iterations with no change in exemplars that stops the convergence, *same_exemplar* = 15.

Given that the ground truth for the clustering is unknown, this paper employs two widely-used metrics suitable for situations like this to assess the performance of the clustering. The first is the average silhouette coefficient (ASC [51]), *ASC* defined as follows,

Algorithm 2 Affinity Propagation Clustering
$(S, p, \lambda, max\_iter, conv\_iter)$

$\qquad num\_iter \leftarrow 1$
$\qquad same\_exemplar\_iter \leftarrow 0$
3: **while** True **do**
$\qquad$ Compute responsibilities based on (18)
$\qquad$ Computer availabilities based on (19)
6: **if** exemplars changed **then**
$\qquad\qquad same\_exemplar\_iter \leftarrow 0$
$\qquad$ **else**
9: $\qquad\qquad same\_exemplar\_iter \leftarrow same\_exemplar\_iter + 1$
$\qquad$ **end if**
$\qquad num\_iter > max\_iter$ or $same\_exemplar\_iter > conv\_iter$ **then**
12: $\qquad$ break
$\qquad$ **end if**
$\qquad num\_iter \leftarrow num\_iter + 1$
15: **end while**
$\qquad$ Find exemplars and assign each data point to the nearest exemplar to finalize clusters

---

$$ASC = \frac{1}{N} \sum_i^N \frac{b_i - a_i}{\max(a_i, b_i)} \qquad (20)$$

where N is the number of samples, and $N = 477$ in this study; a_i is the mean DTW distance between sample i and all other samples in the same cluster; b_i is the mean dynamic warping distance between sample i and all other samples in the next nearest cluster.

A higher ASC score means a model with better-defined clusters. The range is between -1 for incorrect clustering and $+1$ for highly dense clustering, and a score around zero indicates the clusters have too much overlap.

The second measurement of clustering performance is the Calinski-Harabasz index (CHI [52]).. For a set of data D of size N, CHI is defined as follows,

$$CHI = \frac{tr(B_k)}{tr(W_k)} \times \frac{N - k}{k - 1}, \qquad (21)$$

$$B_k = \sum_{q=1}^{k} n_q (c_q - c_D)(c_q - c_D)^T, \qquad (22)$$

$$W_k = \sum_{q=1}^{k} \sum_{x \in C_q} (x - c_q)(x - c_q)^T. \qquad (23)$$

where C_q is the set of points in cluster q; c_q is the center of cluster q; C_D is the set of points in cluster D; and n_q is the number of samples in cluster q.

A higher CHI relates to a more dense and well-separated set of clusters. And both the ASC and the CHI can be evaluated using the machine learning python package, scikit-learn (53), with a precomputed similarity matrix using DTW analysis presented in the previous subsection.

Results

The primary goal of this study is to categorize discretionary lane-changing behaviors. The methodologies presented in the previous sections facilitate a nuanced analysis of lane-changing behavior patterns, drawing on the principles of similarity measurement and cluster analysis. This section shows the categorization results and interpretation of how discretionary lane-changing should be modeled.

### Characterizing Lane-Changing Decision Based on Gaps

This subsection outlines the process of selecting the optimal parameter for AP clustering. This choice gives rise to a discussion of the implications of the smallest number of clusters in relation to modeling lane-changing behaviors considering driver heterogeneity. The subsection then culminates with a detailed classification and characterization of lane-changing behaviors, considering lead and lag gaps.

The AP clustering algorithm takes a preference value as input to denote the likelihood of a sample being chosen as one of the exemplars, and preference is often defined as an integer multiple of the median of the similarity matrix. Therefore, this paper evaluated the performance score with k-multiple of the median in the similarity matrix defined with lead and lag gaps. k is an integrated value ranging from 1 to 60, and the non-converging cases with some k values are excluded.

In Figure 8, it is observed that a distinct pattern is depicted by the blue solid line: the number of clusters initially decreases from 22 and stabilizes at five as the parameter k increases, employing the DTW distance as the measure of difference. Notably, the cluster count diminishes further to three or four when k exceeds 40. Turning to Figure 9, the two solid lines graphically represent the variation of two performance metrics with changes in k. A conspicuous peak in both metrics suggests an optimal clustering solution when k equals 28. Thus, the preference is selected to be 28 multiplied by the median of the similarity matrix with lead and lag gaps, yielding five clusters for lane-changing gap acceptance. It is important to note that the average CHI shows a marked decrease when k surpasses 40, implying that clustering with fewer than five groups may oversimplify the model and fail to capture essential heterogeneity among drivers.
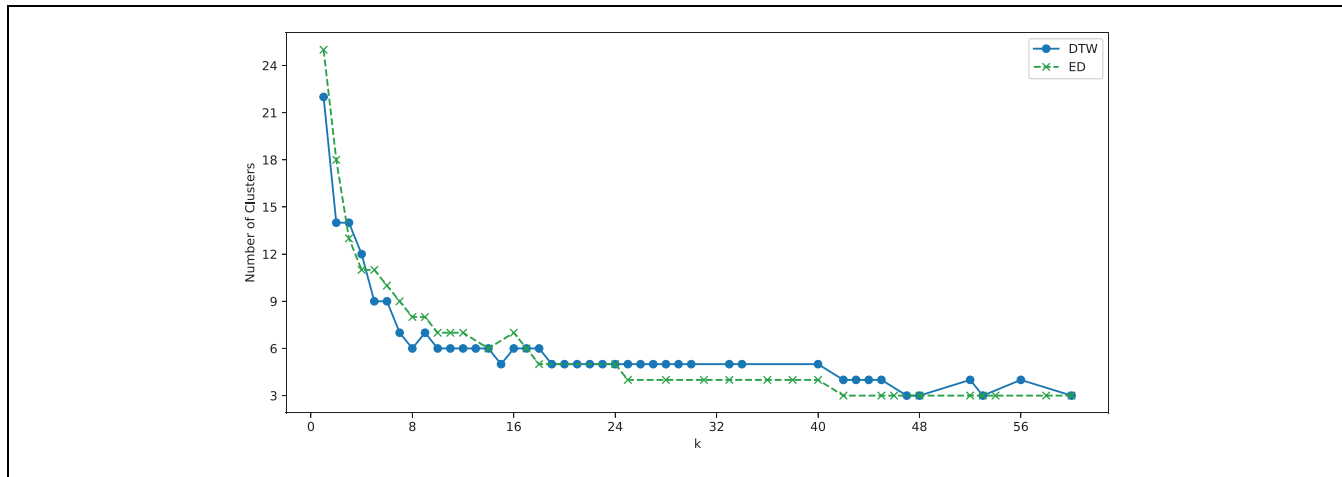
**Figure 8.** Number of clusters based on gaps with different *k* value.
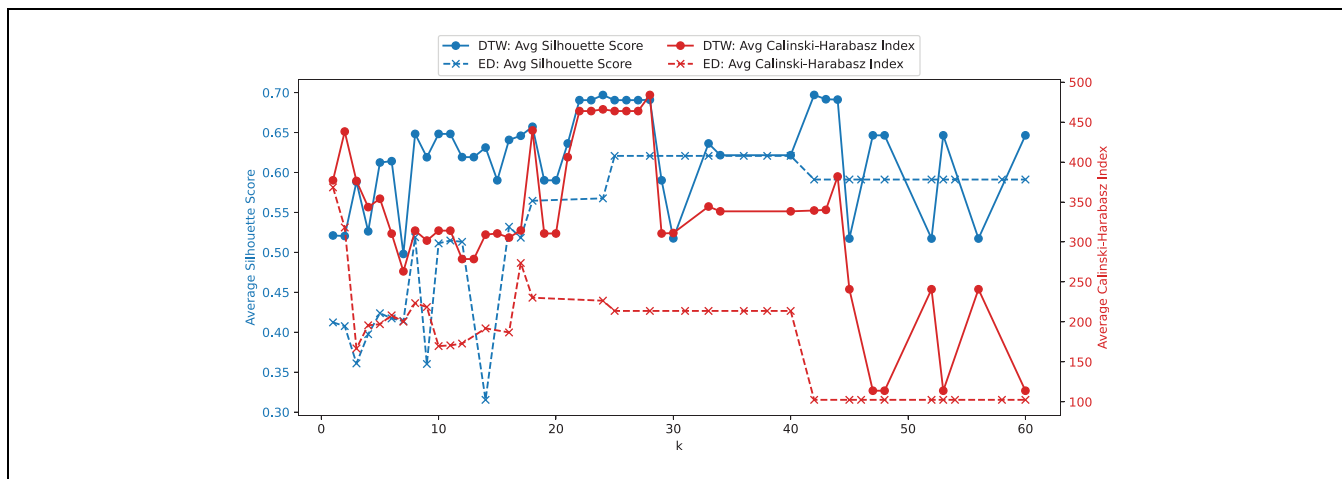
Figure 9. Clustering performance based on gaps with different *k* value.

Similarly, when employing ED as the metric for the similarity matrix, as depicted by the green dashed line in Figure 8, results showed that the number of clusters stabilizes at four when *k* exceeds 25, eventually reducing to three as *k* surpasses 42. Correspondingly, Figure 9 reveals that *k* = 25 is the jointly optimal value for the ASC and the average CHI.

A comparative analysis of the red lines in both figures indicates a consistently higher average CHI when utilizing DTW distance, suggesting that DTW-based clustering may yield more distinct cluster separations. Additionally, the blue lines in Figure 8 demonstrate that the ASC is greater when using ED for clustering at *k* ≤ 29. However, in the few instances where DTW distance does not provide an advantage in the ASC, there is a significant decrease in the average CHI. This scenario should be cautiously avoided. Consequently, these findings suggest that DTW distance may facilitate the formation of denser and better-separated clusters.

Figure 10 presents the joint and marginal distributions of the five clusters based on the DTW distance. The discretionary lane-changing lead gaps can be categorized into three distinct regions: (i) aggressive: 0 to 4 s; (ii) neutral: 4 to 8 s; and (iii) cautious: greater than 8 s. Similarly, the lag gaps can also be segmented into three zones: (i) aggressive: 0 to 2.5 s; (ii) neutral: 2.5 to 7.5 s; and (iii) cautious: greater than 7.5 s. From this, the five clusters within the discretionary lane-changing gaps can be interpreted. Cluster 1 represents aggressive lane-changing behavior in both leading and following directions. While Clusters 2 and 5 exhibit aggressive behavior in the lag gaps, they are neutral and cautious, respectively, when selecting lead gaps. Conversely, Clusters 4 and 3 embody lane-changing behaviors that are aggressive in lead gap selection but neutral and cautious, respectively, on the following end.

Figure 11 presents the clustering outcomes using the ED, where the parameter *k* is set to its optimal value
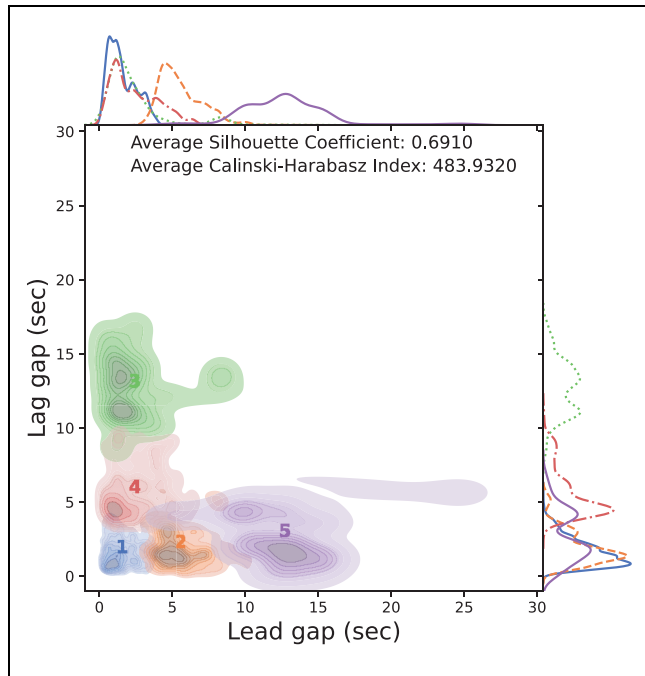
Figure 10. Clustering results on lead and lag gap based on the dynamic time warping (DTW) distance with I-294 dataset in third generation simulation (TGSIM).
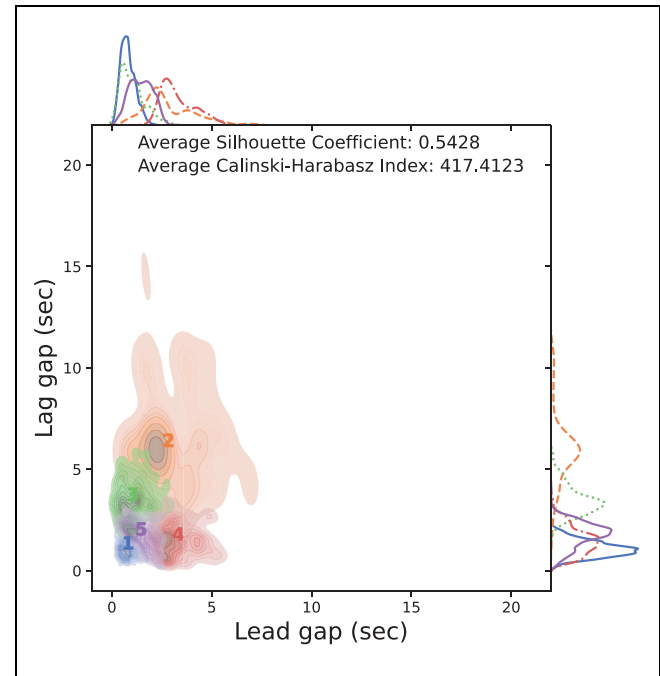

Figure 12. Clustering results on lead and lag gap based on the dynamic time warping (DTW) distance with US-101 dataset in Next Generation Simulation (NGSIM).
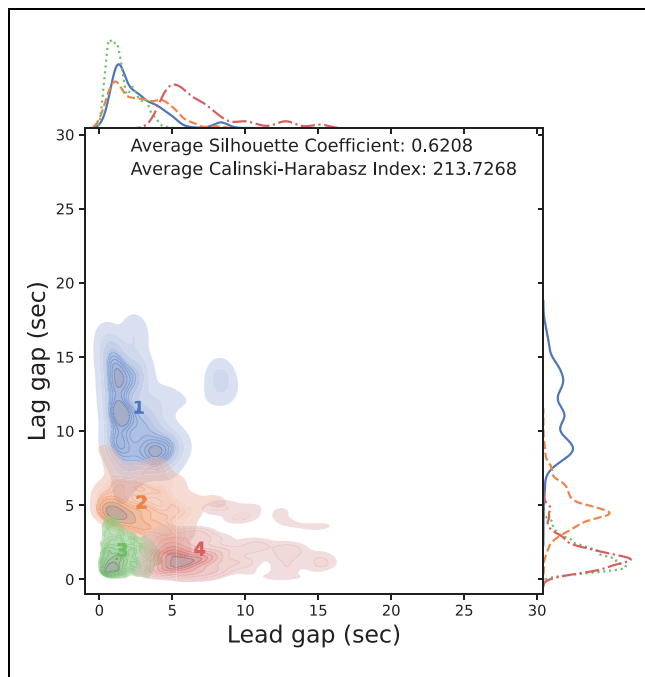

Figure 11. Clustering results on lead and lag gap based on the Euclidean distance (ED) with I-294 dataset dynamic time warping (DTW).

(i.e., $k = 25$). In this configuration, both the average Silhouette Coefficient and the Calinski-Harabasz Index register lower values compared with the scenarios where the DTW distance is employed in the similarity matrix. A notable limitation observed in these results is the inability to differentiate the 'cautious' and 'neutral' categories in the lead gaps.

To validate and verify the effectiveness of the proposed clustering method, a comparative study is conducted on the US-101 dataset from NGSIM (*25*). Figure 12 shows the clustering results using the US-101 dataset from NGSIM, utilizing the same framework, optimized with a clustering parameter of 57, and based on DTW distance for clustering lead and lag gaps. While the clustering analysis revealed five clusters for both datasets, the TGSIM dataset exhibited higher clustering performance, as evidenced by higher cohesion and separation metrics, including the ASCs (*51*) and CHI (*52*). This suggests that the TGSIM data might provide more distinct and separable clusters. Additionally, we observe more variation in the lead gap distribution of TGSIM, which may indicate that TGSIM captures a wider range of lane-changing behaviors under various traffic states, especially in less congested environments, compared with NGSIM.
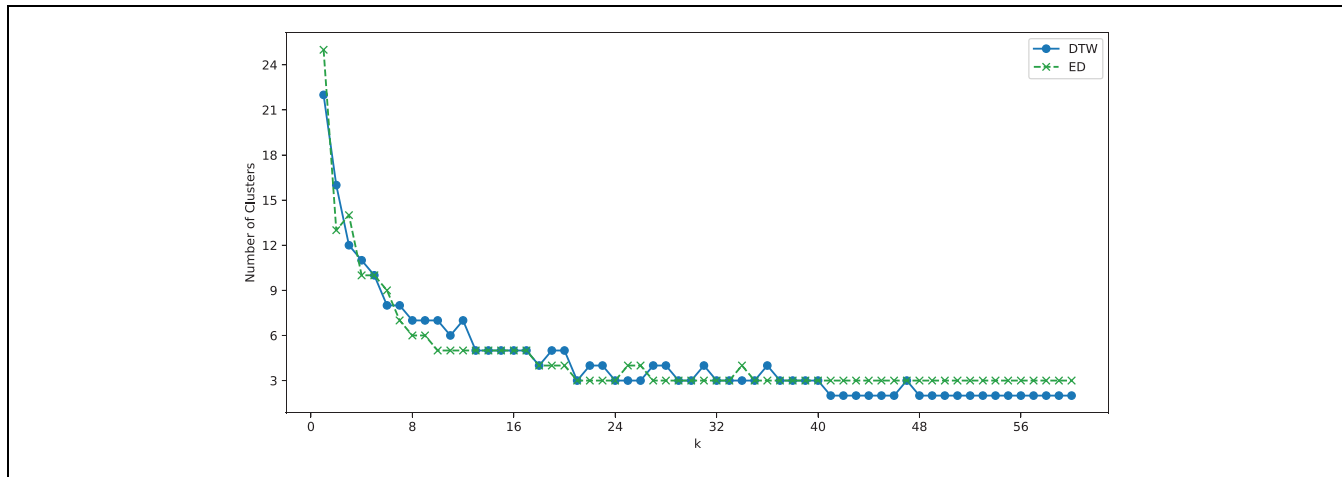
Figure 13. Number of clusters based on relative speeds with different *k* value.
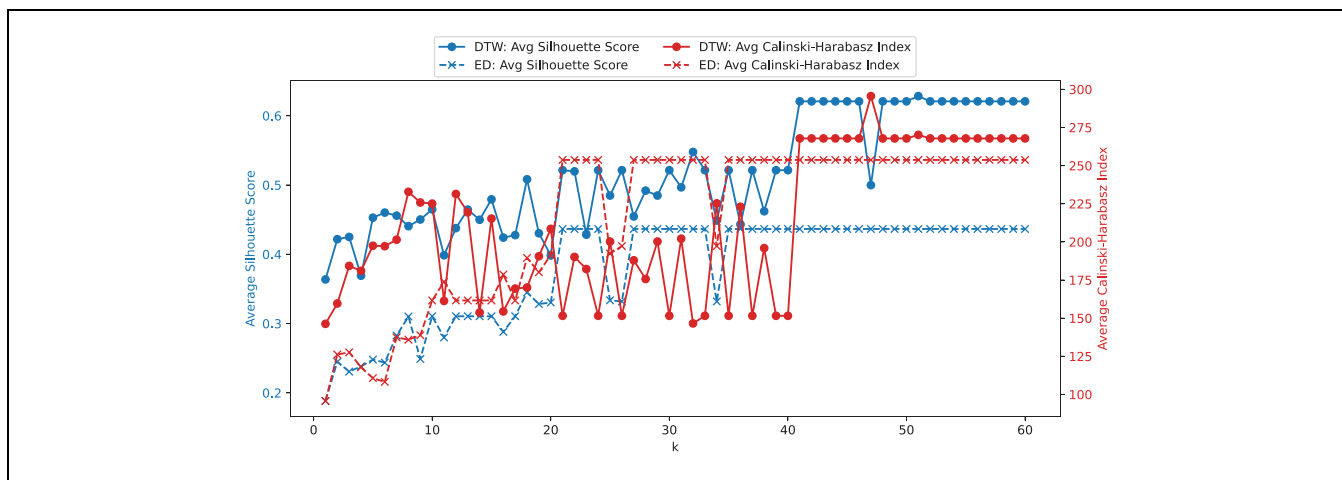
**Figure 14.** Clustering performance based on relative speeds with different *k* value.

Characterizing Lane-Changing Decision Based on Relative Speeds

Employing a methodology analogous to the one used in AP clustering for lead and lag gaps, we observe the variation in the number of clusters as a function of the parameter k. As depicted in Figure 13, this number exhibits a decreasing trend with increasing k, eventually stabilizing at two clusters for $k \geqslant 39$ when using DTW distance, and at three clusters for $k \geqslant 21$ when employing ED as the similarity metric.

In Figure 14, the two solid lines represent the clustering performance metrics for the DTW distance. These lines illustrate a significant enhancement in clustering performance for k values exceeding 40. Consequently, $k = 52$ is identified as the optimal value, yielding two distinct clusters based on relative speeds in the leading and following directions. Conversely, the two dashed lines in the same figure, representing the clustering scores with ED, demonstrate a consistent increase and stabilization for $k \geqslant 21$, peaking at $k = 24$ and resulting in three clusters.

A comparative analysis of the two blue lines in Figure 14 reveals that the ASC is consistently higher for clusters formed using DTW distance, indicating a more effective separation than with ED. Similarly, the red lines show that, while the average CHI experiences fluctuations for k values between 20 and 40 when using DTW, it significantly increases and stabilizes at a higher value compared with ED for $k \geqslant 41$. These observations collectively suggest that employing DTW distance as the metric significantly enhances the categorization of distinct driving behaviors in time series data by more effectively capturing the matching patterns among relative speed time series.
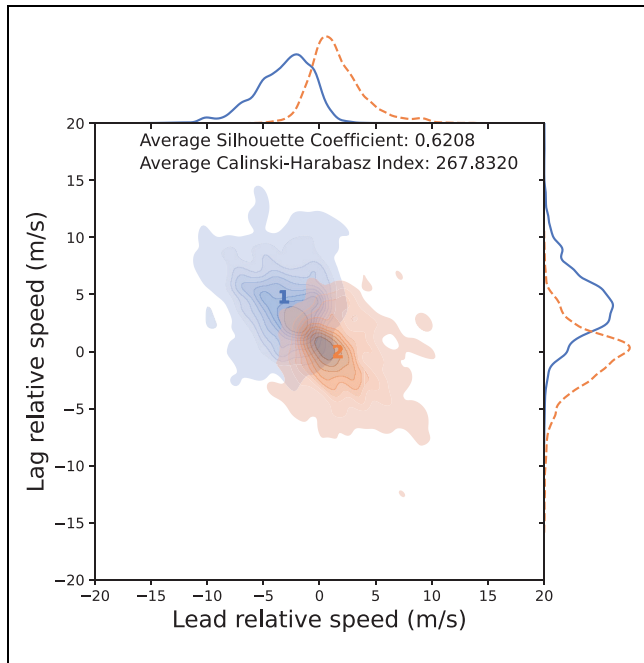
Figure 15. Clustering results on relative speeds based on the dynamic time warping (DTW) distance with I-294 dataset in third generation simulation (TGSIM).
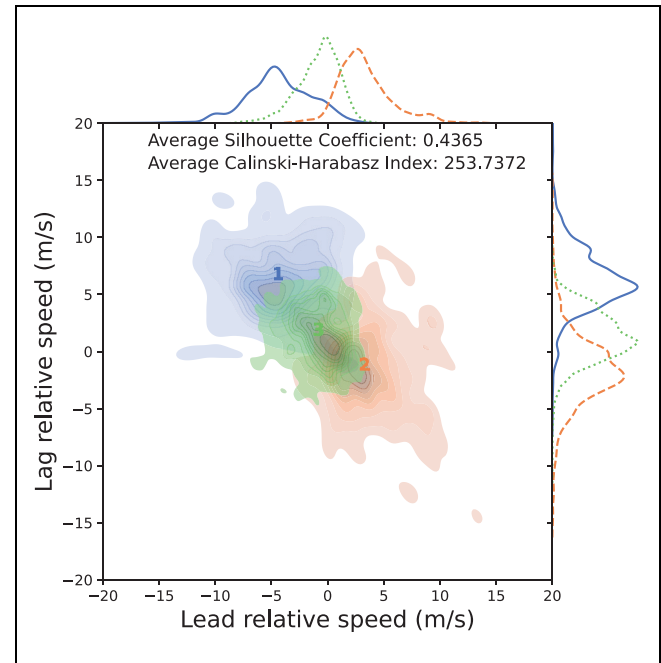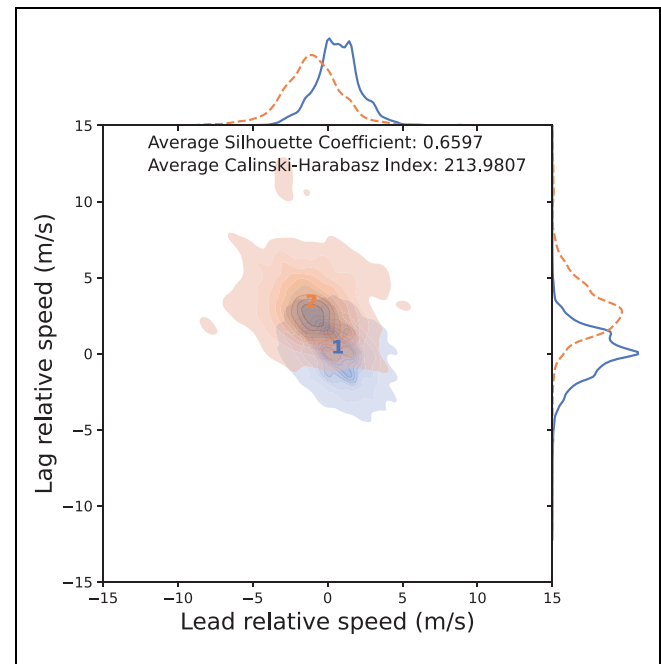

Figure 16. Clustering results on relative speeds based on the Euclidean distance (ED) with I-294 dataset in third generation simulation (TGSIM).

Figure 15 illustrates the joint and marginal distributions for two clusters categorized based on the relative speeds in lead and lag scenarios. Cluster 1 is characterized by a combination of negative lead relative speed and positive lag relative speed. This pattern is indicative of a driving behavior where the driver is overtaking the following vehicle in the target lane. In contrast, Cluster 2 encapsulates scenarios where both lead and lag relative speeds are close to zero, suggesting a lane-changing vehicle maintaining speed parity with surrounding vehicles in the target lane.

Further insights are provided when comparing with Figure 16, which displays the clustering outcomes using ED as the metric of differentiation. In this instance, the result forms three clusters. However, the clustering scores for ED are observed to be lower compared with those obtained using DTW distance. Additionally, the third cluster does not exhibit distinct characteristics when compared with the other two, leading to less discernible differentiation. This outcome reinforces the strength of DTW distance in constructing the similarity matrix for clustering purposes, particularly in effectively distinguishing unique driving behaviors within time series data.

Figure 17 shows the clustering results based on relative speeds for the US-101 dataset from NGSIM. Using the same analysis framework, the clustering parameter is optimized at 91. Both the clustering analyses with NGSIM and TGSIM data yield two clusters. One cluster

Figure 17. Clustering results on relative speeds based on the dynamic time warping (DTW) distance with US-101 dataset in Next Generation Simulation (NGSIM).

corresponds to lane-changing vehicles with near-zero relative speeds for both the lead and lag vehicles in the

target lane, indicating that the lane-changing vehicle maintains a similar speed to the vehicles around it. The other cluster consists of lane-changing vehicles with negative lead and positive lag relative speeds, suggesting that the lane-changing vehicle is moving faster than both the lead and lag vehicles in the target lane.

These findings indicate that the similarity measurement derived from DTW analysis and AP proposed in the methodology section indeed offers an advantage in yielding insights into discretionary lane-changing behaviors.

Conclusions

In conclusion, this study has shown that a data-driven approach can significantly enhance our understanding of discretionary lane-changing behaviors. The lack of high-resolution data to accurately capture lateral movements has long been an impediment to achieving meaningful insight into these behaviors. However, by leveraging the TGSIM dataset, our research provides a breakthrough in this area.

This study first developed a discretionary lane-changing extraction pipeline and conducted a descriptive investigation of critical factors such as gaps and relative speeds. Hypothesis tests were conducted to determine whether gaps and relative speeds should be split into leading and following directions, and results show that analyzing leading and following separately is necessary for modeling lane-changing behaviors.

Therefore, our methodological design employing DTW analysis and AP clustering offers a robust approach to scrutinizing and quantifying driving dynamics in discretionary lane-changing. The DTW analysis plays a pivotal role in quantifying the differences between an array of lane-changing behaviors, and subsequently, the AP clustering allows us to delve deeper into categorizing and characterizing discretionary lane changes.

For the evaluation of clustering performance and the selection of the optimal hyperparameter, two metrics are employed: ASC and CHI. The emergence of five distinct clusters from the data underscores the effectiveness of our methodology, particularly in categorizing lane-changing behaviors into aggressive, neutral, and cautious types in both leading and following directions. Our analysis also revealed two distinctive groups based on relative speeds, one representing overtaking and the other depicting a transition into a lane with stable and homogeneous speed.

Our study's data-driven framework allows for a nuanced examination of discretionary lane-changing behaviors, which is particularly pertinent given the diverse strategies drivers employ on freeways. These strategies, as outlined by Keyvan-Ekbatani et al. (*19*), range from speed leading to traffic leading, each with its unique rationale that may not always align with other drivers' perceptions. Our findings resonate with this concept by identifying specific patterns through high-resolution trajectory data. The emergence of distinct clusters within our dataset corresponds to the diverse lane-changing strategies reported, illustrating a convergence between observed behavior and driver-reported strategies. Notably, our results corroborate the assertion that drivers' lane-changing decisions are multifaceted and extend beyond mere gap acceptance or relative speeds. By leveraging the TGSIM dataset, we shed light on the complexity of driving behaviors and provide empirical support for the various strategies drivers use, which are often influenced by the vehicles' relative positions and speeds.

To summarize, our research has illustrated that the combination of DTW analysis and AP clustering offers a versatile toolset for exploring driving behavior. The inherent adaptability of this approach holds promise for a multitude of contexts. Coupled with providing a more abundant and accurate data set, it could mark the advent of a new era in data-centric research in the realm of traffic flow studies.

Moving forward, it would be worthwhile to extend this study to incorporate aspects such as automated lane-changing and the spatial trajectories in two dimensions associated with lane changes. This will provide a more comprehensive understanding of driving behaviors.

Author Contributions

The authors confirm contribution to the paper as follows: study conception and design: Y. Zhang, A. Talebpour, H. S. Mahmassani and S. Hamdar; data collection: Y. Zhang, A. Talebpour, H. S. Mahmassani and S. Hamdar; analysis and interpretation of results: Y. Zhang, A. Talebpour, H. S. Mahmassani and S. Hamdar; draft manuscript preparation: Y. Zhang, A. Talebpour, H. S. Mahmassani and S. Hamdar. All authors reviewed the results and approved the final version of the manuscript.

Declaration of Conflicting Interests

The author(s) declared no potential conflicts of interest with respect to the research, authorship, and/or publication of this article.

Funding

ORCID iDs

Yanlin Zhang ⓘ https://orcid.org/0000-0002-5342-2755
Alireza Talebpour ⓘ https://orcid.org/0000-0002-5412-5592
Hani S. Mahmassani ⓘ https://orcid.org/0000-0002-8443-8928
Samer H. Hamdar ⓘ https://orcid.org/0000-0001-6896-367X

References

1. Zheng, Z. Recent Developments and Research Needs in Modeling Lane Changing. *Transportation Research Part B: Methodological*, Vol. 60, 2014, pp. 16–32.
2. Pande, A., and M. Abdel-Aty. Assessment of Freeway Traffic Parameters Leading to Lane-Change Related Collisions. *Accident Analysis & Prevention*, Vol. 38, No. 5, 2006, pp. 936–948.
3. van Winsum, W., D. De Waard, and K. A. Brookhuis. Lane Change Manoeuvres and Safety Margins. *Transportation Research Part F: Traffic Psychology and Behaviour*, Vol. 2, No. 3, 1999, pp. 139–149.
4. Kerner, B. S., and H. Rehborn. Experimental Features and Characteristics of Traffic Jams. *Physical Review E*, Vol. 53, No. 2, 1996, p. R1297.
5. Mauch, M., and M. J. Cassidy. Freeway Traffic Oscillations: Observations and Predictions. In *Transportation and Traffic Theory in the 21st Century: Proceedings of the 15th International Symposium on Transportation and Traffic Theory*, Adelaide, Australia, July 16–18, 2002, Emerald Group Publishing Limited, Leeds, 2002, pp. 653–673.
6. Ahn, S., and M. J. Cassidy. Freeway Traffic Oscillations and Vehicle Lane-Change Maneuvers. *Transportation and Traffic Theory*, Vol. 1, 2007, pp. 691–710.
7. Zheng, Z., S. Ahn, D. Chen, and J. Laval. Freeway Traffic Oscillations: Microscopic Analysis of Formations and Propagations Using Wavelet Transform. *Procedia-Social and Behavioral Sciences*, Vol. 17, 2011, pp. 702–716.
8. Cassidy, M. J., and J. Rudjanakanoknad. Increasing the Capacity of an Isolated Merge by Metering Its On-Ramp. *Transportation Research Part B: Methodological*, Vol. 39, No. 10, 2005, pp. 896–913.
9. Yang, Q. I., and H. N. Koutsopoulos. A Microscopic Traffic Simulator for Evaluation of Dynamic Traffic Management Systems. *Transportation Research Part C: Emerging Technologies*, Vol. 4, No. 3, 1996, pp. 113–129.
10. Gipps, P. G. A Behavioural Car-Following Model for Computer Simulation. *Transportation Research Part B: Methodological*, Vol. 15, No. 2, 1981, pp. 105–111.
11. Kesting, A., M. Treiber, and D. Helbing. General Lane-Changing Model MOBIL for Car-Following Models. *Transportation Research Record: Journal of the Transportation Research Board*, 2007. 1999: 86–94.
12. Treiber, M., A. Hennecke, and D. Helbing. Congested Traffic States in Empirical Observations and Microscopic Simulations. *Physical Review E*, Vol. 62, No. 2, 2000, p. 1805.
13. Ahmed, K., M. Ben-Akiva, H. Koutsopoulos, and R. Mishalani. Models of Freeway Lane Changing and Gap Acceptance Behavior. *Transportation and Traffic Theory*, Vol. 13, 1996, pp. 501–515.
14. Toledo, T., H. N. Koutsopoulos, and M. Ben-Akiva. Integrated Driving Behavior Modeling. *Transportation Research Part C: Emerging Technologies*, Vol. 15, No. 2, 2007, pp. 96–112.
15. Kita, H. A Merging–Giveway Interaction Model of Cars in a Merging Section: A Game Theoretic Analysis. *Transportation Research Part A: Policy and Practice*, Vol. 33, No. 3–4, 1999, pp. 305–312.
16. Ban, J. X. A Game Theoretical Approach for Modelling Merging and Yielding Behaviour at Freeway On-Ramp Sections. In *Transportation and Traffic Theory: Papers Selected for Presentation at 17th International Symposium on Transportation and Traffic Theory, a Peer Reviewed Series Since 1959*, Elsevier, Amsterdam, The Netherlands, 2007, p. 197.
17. Talebpour, A., H. S. Mahmassani, and S. H. Hamdar. Modeling Lane-Changing Behavior in a Connected Environment: A Game Theory Approach. *Transportation Research Procedia*, Vol. 7, 2015, pp. 420–440.
18. Ali, Y., Z. Zheng, M. M. Haque, and M. Wang. A Game Theory-Based Approach for Modelling Mandatory Lane-Changing Behaviour in a Connected Environment. *Transportation Research Part C: Emerging Technologies*, Vol. 106, 2019, pp. 220–242.
19. Keyvan-Ekbatani, M., V. L. Knoop, and W. Daamen. Categorization of the Lane Change Decision Process on Freeways. *Transportation Research Part C: Emerging Technologies*, Vol. 69, 2016, pp. 515–526.
20. Knoop, V., M. Keyvan-Ekbatani, M. de Baat, H. Taale, and S. Hoogendoorn. Lane Change Behavior on Freeways: An Online Survey Using Video Clips. *Journal of Advanced Transportation*, Vol. 2018, 2018, p. 9236028.
21. Zhang, Y., Y. Zou, Y. Xie, and L. Chen. Identifying Dynamic Interaction Patterns in Mandatory and Discretionary Lane Changes Using Graph Structure. *Computer-Aided Civil and Infrastructure Engineering*, Vol. 39, No. 5, 2024, pp. 638–655.
22. Zhang, Y., and A. Talebpour. Characterizing Human–Automated Vehicle Interactions: An Investigation into Car-Following Behavior. *Transportation Research Record: Journal of the Transportation Research Board*, 2024; 2678: 812–826.
23. Yang, M., X. Wang, and M. Quddus. Examining Lane Change Gap Acceptance, Duration and Impact Using Naturalistic Driving Data. *Transportation Research Part C: Emerging Technologies*, Vol. 104, 2019, pp. 317–331.
24. Das, A., M. N. Khan, and M. M. Ahmed. Nonparametric Multivariate Adaptive Regression Splines Models for Investigating Lane-Changing Gap Acceptance Behavior Utilizing Strategic Highway Research Program 2 Naturalistic Driving Data. *Transportation Research Record: Journal of the Transportation Research Board*, 2020. 2674: 223–238.
25. *Next Generation Simulation: US101 Freeway Dataset*. Federal Highway Administration, Washingtion, D.C., 2007.
26. Gloudemans, D., Y. Wang, J. Ji, G. Zachar, W. Barbour, E. Hall, M. Cebelak, L. Smith, and D. B. Work. I-24 MOTION: An Instrument for Freeway Traffic Science. *Transportation Research Part C: Emerging Technologies*, Vol. 155, 2023, p. 104311.

27. Wang, Q., Z. Li, and L. Li. Investigation of Discretionary Lane-Change Characteristics Using Next-Generation Simulation Data Sets. *Journal of Intelligent Transportation Systems*, Vol. 18, No. 3, 2014, pp. 246–253.

28. Li, L., C. Lv, D. Cao, and J. Zhang. Retrieving Common Discretionary Lane Changing Characteristics from Trajectories. *IEEE Transactions on Vehicular Technology*, Vol. 67, No. 3, 2017, pp. 2014–2024.

29. Coifman, B., and L. Li. A Critical Evaluation of the Next Generation Simulation (NGSIM) Vehicle Trajectory Dataset. *Transportation Research Part B: Methodological*, Vol. 105, 2017, pp. 362–377.

30. Krajewski, R., J. Bock, L. Kloeker, and L. Eckstein. The highD Dataset: A Drone Dataset of Naturalistic Vehicle Trajectories on German Highways for Validation of Highly Automated Driving Systems. *Proc., 2018 21st International Conference on Intelligent Transportation Systems (ITSC)*, 2018, pp. 2118–2125. New York: IEEE.

31. Barmpounakis, E., and N. Geroliminis. On the New Era of Urban Traffic Monitoring with Massive Drone Data: The pNEUMA Large-Scale Field Experiment. *Transportation Research Part C: Emerging Technologies*, Vol. 111, 2020, pp. 50–71.

32. Ammourah, R., P. Beigi, B. Fan, H. S. H., R. James, M. Khajeh-Hosseini, H. S. Mahmassani, D. Monzer, A. Talebpour, Y. Zhang, T. Radvand, and C.-C. Hsiao, Introduction to the Third Generation Simulation (TGSIM) Dataset: Data Collection and Trajectory Extraction. Transportation Research Record, 2024, p. 03611981241257257.

33. Ali, Y., Z. Zheng, and M. C. Bliemer. Calibrating Lane-Changing Models: Two Data-Related Issues and a General Method to Extract Appropriate Data. *Transportation Research Part C: Emerging Technologies*, Vol. 152, 2023, p. 104182.

34. Laval, J. A. Self-organized Criticality of Traffic Flow: Implications for Congestion Management Technologies. *Transportation Research Part C: Emerging Technologies*, Vol. 149, 2023, p. 104056.

35. Clauset, A., C. R. Shalizi, and M. E. Newman. Power-Law Distributions in Empirical Data. *SIAM Review*, Vol. 51, No. 4, 2009, pp. 661–703.

36. Alstott, J., E. Bullmore, and D. Plenz. Powerlaw: A Python Package for Analysis of Heavy-Tailed Distributions. *PLoS One*, Vol. 9, No. 1, 2014, p. e85777.

37. Wilcoxon, F. Individual Comparisons by Ranking Methods. In *Breakthroughs in Statistics: Methodology and Distribution* (S. Kotz, and N. L. Johnson, eds.), Springer, New York, NY, 1992, pp. 196–202.

38. Goswami, A., W. Han, Z. Wang, and A. Jiang. Controlled Experiments for Decision-Making in e-Commerce Search. *Proc., 2015 IEEE International Conference on Big Data (Big Data)*, IEEE, New York, 2015, pp. 1094–1102.

39. Bellman, R., and R. Kalaba. On Adaptive Control Processes. *IRE Transactions on Automatic Control*, Vol. 4, No. 2, 1959, pp. 1–9.

40. Myers, C., L. Rabiner, and A. Rosenberg. Performance Tradeoffs in Dynamic Time Warping Algorithms for Isolated Word Recognition. *IEEE Transactions on Acoustics, Speech, and Signal Processing*, Vol. 28, No. 6, 1980, pp. 623–635.

41. Sakoe, H., and S. Chiba. Dynamic Programming Algorithm Optimization for Spoken Word Recognition. *IEEE Transactions on Acoustics, Speech, and Signal Processing*, Vol. 26, No. 1, 1978, pp. 43–49.

42. Hosseini, M. K., A. Talebpour, S. Devunuri, and S. H. Hamdar. An Unsupervised Learning Framework for Detecting Adaptive Cruise Control Operated Vehicles in a Vehicle Trajectory Data. *Expert Systems with Applications*, Vol. 208, 2022, p. 118060.

43. Rakthanmanon, T., B. Campana, A. Mueen, G. Batista, B. Westover, Q. Zhu, J. Zakaria, and E. Keogh. Searching and Mining Trillions of Time Series Subsequences Under Dynamic Time Warping. In *Proceedings of the 18th ACM SIGKDD International Conference on Knowledge Discovery and Data Mining*, Beijing, China, Association for Computing Machinery, New York, 2012, pp. 262–270.

44. Senin, P. Dynamic Time Warping Algorithm Review. Information and Computer Science Department University of Hawaii at Manoa Honolulu, USA, Vol. 855, 2008, pp. 1–23.

45. MacQueen, J. Some Methods for Classification and Analysis of Multivariate Observations. *Proc., 5th Berkeley Symposium on Mathematical Statistics and Probability*, Oakland, CA, University of California Press, Berkeley, CA, 1967, Vol. 1, pp. 281–297.

46. Shi. Multiclass Spectral Clustering. *Proc., 9th IEEE International Conference on Computer Vision*, IEEE, New York, 2003, pp. 313–319.

47. Ester, M., H.-P. Kriegel, J. Sander, and X. Xu. A Density-Based Algorithm for Discovering Clusters in Large Spatial Databases with Noise. *kdd*, Vol. 96, 1996, pp. 226–231.

48. Frey, B. J., and D. Dueck. Clustering by Passing Messages Between Data Points. *science*, Vol. 315, No. 5814, 2007, pp. 972–976.

49. Akl, A., and S. Valaee. Accelerometer-Based Gesture Recognition via Dynamic-Time Warping, Affinity Propagation, & Compressive Sensing. *Proc., 2010 IEEE International Conference on Acoustics, Speech and Signal Processing*, IEEE, New York, 2010, pp. 2270–2273.

50. Mézard, M. Where Are the Exemplars? *Science*, Vol. 315, No. 5814, 2007, pp. 949–951.

51. Rousseeuw, P. J. Silhouettes: A Graphical Aid to the Interpretation and Validation of Cluster Analysis. *Journal of Computational and Applied Mathematics*, Vol. 20, 1987, pp. 53–65.

52. Caliński, T., and J. Harabasz. A Dendrite Method for Cluster Analysis. *Communications in Statistics-Theory and Methods*, Vol. 3, No. 1, 1974, pp. 1–27.

53. Pedregosa, F., G. Varoquaux, A. Gramfort, V. Michel, B. Thirion, O. Grisel, M. Blondel, et al. Scikit-Learn: Machine Learning in Python. *Journal of Machine Learning Research*, Vol. 12, 2011, pp. 2825–2830.